Title

Versatile tuning of supramolecular hydrogels through metal complexation of oxidation-resistant catechol-inspired ligands

Journal

Soft Matter, 9(43)

ISSN

1744-683X

Authors

Menyo, Matthew S
Hawker, Craig J
Waite, J Herbert

Publication Date

2013

DOI

10.1039/c3sm51824h

Peer reviewed

Soft Matter

RSC Publishing

PAPER

View Article Online
View Journal | View Issue

Cite this: *Soft Matter*, 2013, **9**, 10314

Versatile tuning of supramolecular hydrogels through metal complexation of oxidation-resistant catechol-inspired ligands†

Matthew S. Menyo,[a] Craig J. Hawker*[b] and J. Herbert Waite*[ac]

Received 3rd July 2013
Accepted 19th September 2013

DOI: 10.1039/c3sm51824h

www.rsc.org/softmatter

The mussel byssal cuticle employs DOPA–Fe^{3+} complexation to provide strong, yet reversible crosslinking. Synthetic constructs employing this design motif based on catechol units are plagued by oxidation-driven degradation of the catechol units and the requirement for highly alkaline pH conditions leading to decreased performance and loss of supramolecular properties. Herein, a platform based on a 4-arm poly(ethylene glycol) hydrogel system is used to explore the utility of DOPA analogues such as the parent catechol and derivatives, 4-nitrocatechol (nCat) and 3-hydroxy-4-pyridinonone (HOPO), as structural crosslinking agents upon complexation with metal ions. HOPO moieties are found to hold particular promise, as robust gelation with Fe^{3+} occurs at physiological pH and is found to be largely resistant to oxidative degradation. Gelation is also shown to be triggered by other biorelevant metal ions such as Al^{3+}, Ga^{3+} and Cu^{2+} which allows for tuning of the release and dissolution profiles with potential application as injectable delivery systems.

Introduction

The remarkable functional behavior of biological materials is enabled by, and intimately coupled to, dynamic structural interactions that occur at multiple length and time scales. As demonstrated by the mechanochemical analysis of titin[1] and spider silk,[2] profoundly useful insights can be distilled from a fundamental understanding of these interactions. In synthetic polymeric systems, dynamic bonding has the ability to expand the range of properties due to the inherent responsiveness to local stimuli and healable nature of these bonds.[3] This dynamic nature is dramatically apparent in polymer hydrogels, where factors such as pH,[4,5] temperature,[6] salt concentration,[7] and light[8–12] can trigger reversible gel formation, dissolution, reshaping, and/or internal healing. A wide variety of supramolecular interactions, including hydrogen bonding,[13,14] hydrophobic effects,[15] π–π stacking,[16] electrostatic attraction,[17,18] and metal–ligand coordination[19–21] have been used to drive assembly.

Individual metal–ligand coordination sites can provide stable, yet reversible, crosslinking points between polymers, in contrast to other mechanisms of dynamic crosslinking, where multiple weak interactions must act in concert to achieve self-supporting gels.[22] One particular metal–ligand interaction observed widely in nature is that of catecholic ligands with Fe(III). The coordination of ferric iron with enterobactin (tripodal tris-catecholate siderophore from *E. coli*) has a measured stability constant of 10^{52}, equating to a free energy for the complex 2 orders of magnitude higher than a single hydrogen bond, 3 times as high as the "gold standard" non-covalent interaction of biotin and avidin, and comparable to a covalent bond.[23] Similarly, the cuticle of the mussel byssal thread employs DOPA residues to establish catechol-based, Fe(III) crosslinks in composite systems that arrest crack formation and drive recoverability under the repetitive high strain of waves and tides.[24] In addition to its strength and dynamic nature, catechol–Fe(III) complexation is highly pH-dependent. Binding stoichiometry changes from a 1 : 1 mono complex at low pH to a highly stable 3 : 1 catechol : Fe(III) tris state at increased pH.

While biological systems have evolved to take advantage of the uniquely high affinity of catecholic moieties for Fe(III), the task of implementing catechol–Fe(III) coordination in materials systems is fraught with peril. Catechols are prone to rapid auto-oxidation at neutral to alkaline pH,[25] forming a quinone species which shows significantly reduced affinity for Fe(III) and is susceptible to covalent crosslinking through reaction with a variety of nucleophiles, including catechol itself.[26] Furthermore, complexed Fe(III) can catalyze a one-electron ligand-to-metal charge transfer to generate semiquinone and Fe(II), a process which is greatly accelerated at low pH.[27] This complex can quickly dissociate, in which case Fe(II) typically generates free

[a]*Graduate Program in Biomolecular Science and Engineering, University of California, Santa Barbara, CA 93106, USA. E-mail: herbert.waite@lifesci.ucsb.edu*

[b]*Materials Research Laboratory, University of California, Santa Barbara, CA 93106, USA. E-mail: hawker@mrl.ucsb.edu*

[c]*Marine Science Institute, University of California, Santa Barbara, CA 93106, USA*

† Electronic supplementary information (ESI) available: Multimedia showing injection gelation process, additional dynamic rheological characterization. See DOI: 10.1039/c3sm51824h

radicals *via* a Fenton pathway,[28] while the semiquinone is susceptible to further oxidation resulting in quinone and covalent crosslinking.[29] As a result, the dynamic nature of the catechol–Fe(III) bond is undermined by the very conditions which prompt its utility. Furthermore, achieving tris complexes, responsible for the strongest metal binding, requires highly alkaline conditions, due to strong proton competition for the catecholate ligand. In a simple hydrogel system formed from DOPA-functionalized poly(ethylene glycol) (PEG), Holten-Andersen *et al.* found that substantial tris-catecholate–iron complexation did not occur until pH 8, with complete complex formation requiring pH $\sim$ 12.[19]

Given these limitations and to address the above challenges, alternative chelating functionalities with high coordination affinity, pH-dependent speciation and lower susceptibility to oxidation were examined. Focus was directed to two analogues based on the parent catechol derivative: 4-nitrocatechol (nCat) and 3-hydroxy-4-pyridinone (HOPO), as shown in Fig. 1. These analogues withdraw electron density from the phenolate moieties both inductively and through resonance effects, while maintaining the desired bidentate phenolate nature of the catechol. The net effect manifests in reduced phenolic pK_a values (pK_{a1} HOPO = 3.6, pK_{a1} nCat = 6.6, pK_{a1} catechol = 9.2),[30] increased oxidation potentials, and shifted metal–ligand stoichiometry. Measured stability constants for tris-Fe(III) complexed nCat (log β_3 = 39.2)[30] and HOPO (log β_3 = 37.6)[31] are remarkably high, though slightly lower than catechol (log β_3 = 43) due to the "softer" nature of the phenolate ligands.

A 4-arm PEG backbone, where each chain end is functionalized with a chelating functional group, was chosen as the scaffold for hydrogel formation. This simple construct allows clear determination of the relationship between metal–ligand coordination and bulk hydrogel properties. The presence of a single chelating functional group at each chain end, rather than multiple moieties interspersed within a domain, is expected to drive "crosslinking" intermolecular coordination rather than "looping" intramolecular complexes, and allow for rapid gel equilibration. This architecture is also advantageous for potential biological application, as the high water content and biocompatibility of PEG-based hydrogels are well established.[32]

Herein, we describe the synthesis and characterization of hydrogels prepared from catechol-, nitrocatechol-, and 3-hydroxy-4-pyridinone-based 4-arm crosslinkers upon complexation with Fe(III) and other metal ions with high affinity for this class of chelators. The mechanical properties of the hydrogels are found to be strongly dependent on pH, preparation conditions, and metal ion identity. HOPO in particular was shown to be particularly attractive as a chelating functionality in this architecture. It is able to rapidly shift to a tris coordinative mode upon exposure to physiological pH buffer, allowing liquid-to-gel transition with limited dissolution of the polymeric crosslinker or leakage of water-soluble cargo, as studied with Acid Red 27 dye. These hydrogels exhibit high stiffness and have long characteristic bond lifetime, leading to gels that behave elastically over a wide range of frequencies. Furthermore, these gels have long-term stability both on the benchtop, where the gels maintain their rheological behavior and dynamic character, and in physiological buffer, where the gels were observed to slowly dissolve over the course of several days. Taken together, these characteristics make HOPO-based hydrogels an appealing target for injectable gelling agents with excellent encapsulation behavior and mechanical properties.

Results and discussion

Synthesis and gelation

A commercial 4-arm PEG–OH derivative (MW: 10 000 Da) was selected as a common platform for chain end functionalization and subsequent hydrogel formation studies. Chain end functionalization was accomplished by initial reaction of the terminal hydroxyl groups with ethyl bromoacetate followed by hydrolysis of the ester groups to yield the desired 4-arm PEG–COOH system with almost quantitative conversion of chain end groups. From this common functional PEG derivative, the different chelating units (dopamine, 6-nitrodopamine, 2-methyl-3-hydroxy-4-pyridinone ethylamine) were attached through an amide coupling reaction with HBTU. Chain end functionalization efficiencies were again shown to be high with 90%, 95%, and 96% conversion being observed respectively which is in agreement with literature results.[34] Hydrogels were

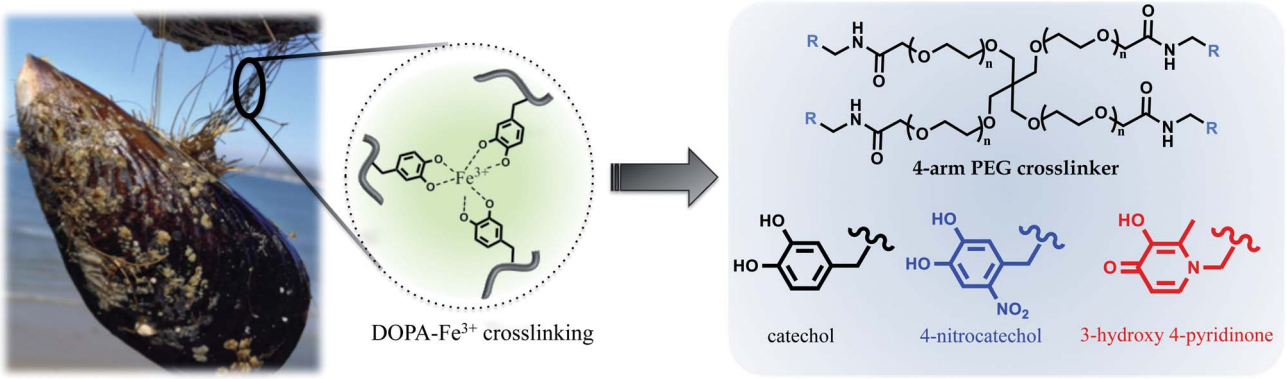

Fig. 1 Cartoon highlighting translation of the strong, healable DOPA–Fe^{3+} crosslinks of the cuticle of *Mytilus californianus*, and the structure of the 4-arm poly(ethylene glycol) (PEG) backbone with pendant catechol (Cat), nitrocatechol (nCat) and 3-hydroxy-4-pyridinone (HOPO) chelating moieties.

then formed through crosslinking metal–ligand coordination between the 3 chelators investigated and metal ions known to exhibit high binding affinities for bidentate catechol ligands. Initial hydrogel formation followed the procedure of Holten-Andersen *et al.*[19]

Briefly, the 4-arm chelator was dissolved in deionized water, and a solution of the metal chloride was added to achieve a 3 : 1 chelator : metal ion ratio. The acidity of the metal salt solution and protons released during chelation ensured predominantly mono-coordination and, as expected, no gelation was observed in these cases. Final gel concentration and pH values was achieved by addition of an appropriate buffer solution, and verified with a pH probe electrode. Gelation is attributed to the pH-driven increase in binding stoichiometry leading to crosslinking bis and tris complexes. For Fe(III)-bound gels, this speciation could conveniently be tracked through distinct spectrophotometric signatures for each stoichiometry. For gels with more labile crosslinks, rigorous mixing led to uniform gels in short order, however for hydroxypyridinone-based gels, which exhibited notably longer effective bond lifetimes, equilibration required long times (~2 hours).

Effect of pH and chelating group

The dynamic mechanical properties of metal–ligand crosslinked hydrogels are determined primarily by the dissociation and reformation of the coordination bonds, though these are difficult to measure quantitatively for high affinity complexes. According to Bell Theory,[35] bond lifetime scales with the exponential of bond energy, however, metal–ligand dissociation dynamics have been shown to dominate the dynamic mechanical properties of lower affinity pincer-Pt/pyridine organogels.[22] Studies of iron dissociation from natural and synthetic siderophores have established that chelator protonation is often the rate-limiting step in the dissociation process of a high affinity Fe(III) complex.[36] While catechol-based derivatives have the highest stability constants with Fe(III), they also have the highest proton affinity, as reflected by phenolic pK_a values (9.1 and 14 for catechol, 6.7 and 10.3 for nitrocatechol, 3.6 and 9.9 for HOPO) and pH-dependent coordination stoichiometry.[30,37,38] Based on these predictive small molecule data, we hypothesized that hydrogels with nitrocatechol and HOPO-based crosslinks would form robust hydrogels at pH values lower and more feasible for biological application than catechol-based gels.

To test this hypothesis, 10% w/v hydrogels were prepared from the same 4-arm PEG backbone with catechol, nitrocatechol and 3-hydroxy-4-pyridinone (HOPO) chain ends and Fe(III) at pH 9. This pH was necessary to yield gelation in the case of catechol-based crosslinkers. Oscillatory rheology (Fig. 2a) was used to probe the dynamic mechanical properties of the hydrogels, and by extension, the nature of the metal–ligand crosslinks. The hydrogels tested show similar plateau moduli around 12 kPa, but characteristic relaxation time τ varied greatly: ≈0.09 seconds for catechol-, ≈8 seconds for nitrocatechol- and >125 seconds for HOPO-based gels. Step-strain experiments (Fig. 2b) show that all freshly synthesized gels exhibit relaxation to a zero stress state after 20% shear strain, indicative of gel networks crosslinked through dynamic and not covalent bonding.

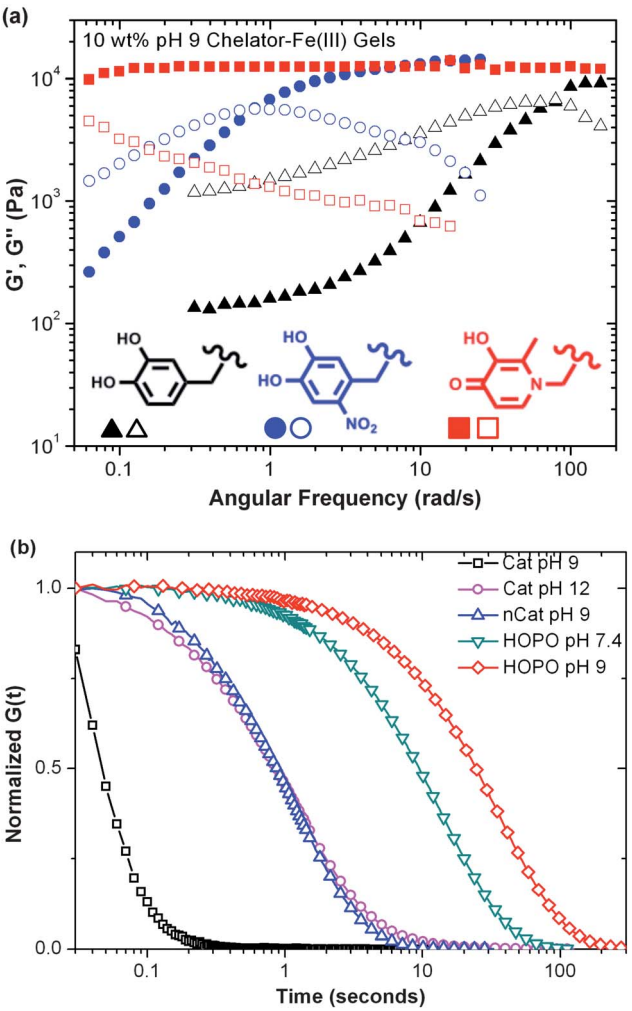

Fig. 2 (a) Frequency sweep of hydrogels at pH 9 with storage (G') and loss (G'') moduli reported as closed and open symbols, respectively. (b) Relaxation of hydrogels after subjection to a 20% shear step strain.

Both nitrocatechol and HOPO-based gels are predominantly tris-coordinate at pH 9, whereas catechol-based gels have a large amount of bis coordination, a supposition supported by spectrophotometric evaluation of the gels in comparison to solutions and published data. Tris complexes are much more stable than complexes of lower stoichiometry; a bis catechol–Fe(III) complex ($\log \beta = 33$) has an associated free energy of complexation almost an order of magnitude lower than that of the tris complex ($\log \beta = 43$), and lower than the stability constants of both nitrocatechol and HOPO tris chelates. Interestingly, catechol-based gels at pH 12 and nitrocatechol-based gels at pH 9, where small molecule speciation plots predict essentially complete tris crosslinking, exhibit notably shorter characteristic relaxation than HOPO-based gels at either pH 7.4 or pH 9. One proposed explanation is that the kinetics of ligand exchange between HOPO–Fe(III) complexes are slower than that of catechol–Fe(III). Additionally, the higher concentration of

hydroxide ions at pH 12 results in increased competition for catechol complexation with Fe(III).

With HOPO identified as a promising crosslinking functionality, the effect of pH on the viscoelastic properties was further investigated. Fig. 3a shows dynamic oscillatory rheology on HOPO–Fe(III) gels synthesized at pH 4.5, 7.4 and 9. As gel pH is raised from 4.5 (a mixture of bis and tris stoichiometry) to 7.4 (predominantly tris-crosslinked), increased elastic character in the gels is readily apparent, though all gels exhibit the same plateau modulus. Fig. 3b highlights the changing absorbance as pH increases from pH 3 to pH 9 in solutions of diluted 4-arm HOPO and that of the gel formed at pH 7.4. Notable are the virtually identical spectra for HOPO solution and gel at 7.4 and 9, confirming unchanged chelation stoichiometry above pH 7.4 in either gel or solution. Absorptions match previously assigned spectrophotometric signatures for HOPO–Fe(III) binding stoichiometries determined for the small molecule deferiprone.[39] Therefore, the increased bond lifetime of hydrogels at pH 9 compared to pH 7.4 is attributed to slower ligand dissociation kinetics due to decreased proton concentration at higher pH values, and not to a change in the degree of coordination.

Supramolecular assembly

The rapid and stable gelation seen for HOPO-based hydrogels at physiological pH strongly suggests that gels could be formed upon injection into a bulk buffer solution. To test this hypothesis, unbuffered polymer solutions with a 3 : 1 chelator : Fe(III) ratio were prepared to the desired final gel concentration and either dropped or injected into a buffer solution at the desired gel pH (7.4 or 9). Indeed, this rapid change in pH led to immediate formation of a distinct hydrogel, as shown in the ESI video (S1).† Injected gels were equilibrated for 30 seconds, removed from the buffer, briefly blotted dry, and weighed. UV-Vis spectroscopy detected no measureable absorption from the high extinction coefficient chelator–metal complex in the buffer solution.

Hydrogels prepared by injection from a 10% w/v polymer solution show virtually identical rheological behavior to those synthesized through the conventional "dilution" approach, as

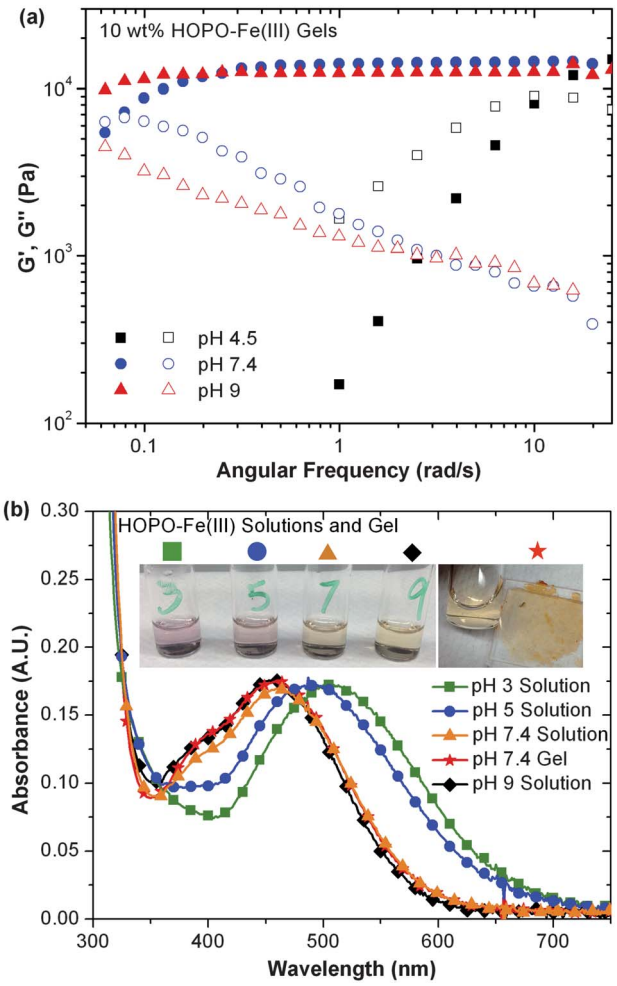

Fig. 3 (a) Effect of pH on rheological behavior of HOPO hydrogels at pH 4.5 (black), 7.4 (blue) and 9 (red) and (b) the absorbance of 1% w/v HOPO crosslinker–Fe^{3+} solutions and 10% w/v hydrogel with annotated photographs.

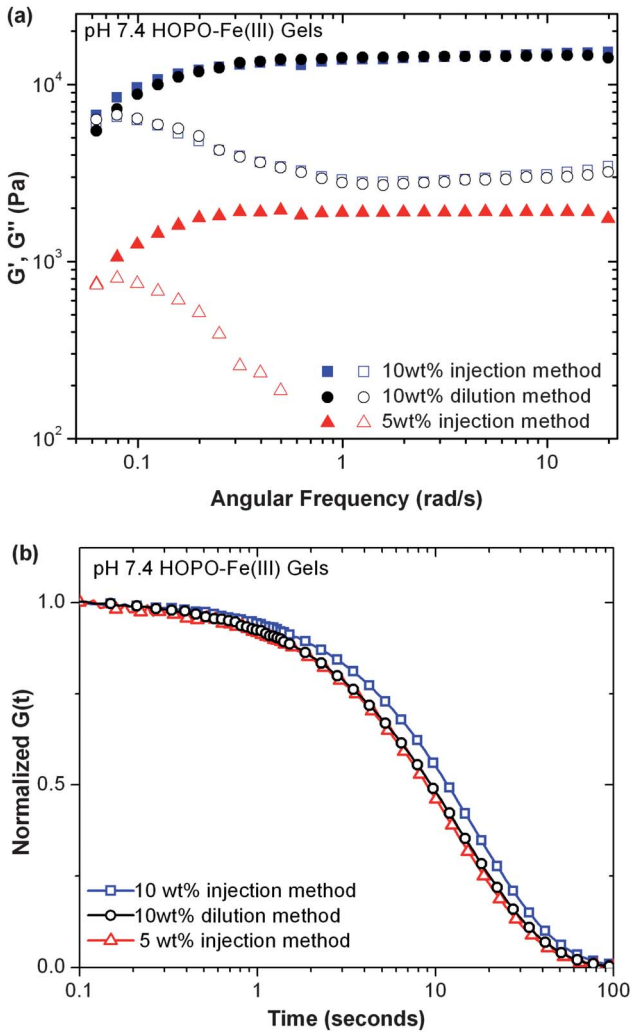

Fig. 4 Effect of hydrogel preparation method and conditions on rheological behavior evaluated by (a) frequency sweep and (b) step strain experiments.

shown in Fig. 4. Furthermore, gels synthesized by injection of a 5% w/v solution had a plateau modulus an order of magnitude lower than those from a 10% w/v solution, though exhibiting similar characteristic bond lifetimes. This suggests that, while the nature of the crosslinks is similar, the initial stiffness and water incorporation of the gels is determined by the injection solution, and hydrogels are not prone to equilibration with the bulk solution over the time frame required for robust gelation. In contrast, catechol and nitrocatechol-based gels showed no gelation upon injection into pH 7.4 buffer solutions, and significant dissolution even into higher pH solutions (12 for catechol and 9 for nitrocatechol) (ESI Fig. S2†).

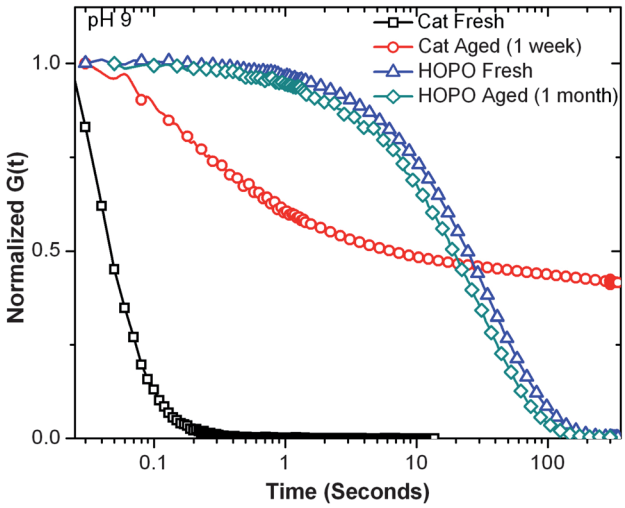

Fig. 6 Relaxation of catechol and HOPO hydrogels after aging under ambient conditions.

Gel stability

In all prior work on catechol-based, supramolecular hydrogels, long-term stability is a major issue. This is due to the relative ease with which catechol groups can be oxidized to quinone, a reactive functionality prone to nucleophilic attack and phenolic coupling reactions to yield covalent crosslinks and loss of supramolecular characteristics.[40] This oxidation can proceed rapidly at neutral to alkaline pH in the absence of oxidizing agents, with only trace amounts of oxygen necessary to trigger this cascade. It is also well described in literature that catechol–Fe(III) complexes are susceptible to a one-electron intracomplex redox process, generating Fe(II) and a semiquinone, which again is susceptible to further oxidation and crosslinking. This process has been thoroughly and eloquently characterized for PEG-based gel systems, and it was shown that 1 : 1 catechol–Fe complexes at low pH values are especially vulnerable.[29]

With this in mind, the long-term stability of the hydrogels synthesized was examined by initially storing a series of catechol–Fe(III) gels, synthesized at pH 9, at room temperature and exposure to light and oxygen for one week. Aging was visually apparent in all samples with the initially wine red gel slowly becoming muddy-brown in color, characteristic of catechol-based oligomerization, with time. UV-visible spectroscopy of the gel and representative solutions initially show a characteristic 3 : 1 catechol–Fe tris complex absorbances of the charge transfer complex ($\lambda_{max} = 480$ nm) and the catechol ($\lambda_{max} = 280$ nm), shifting to a broad, tailing absorbance with $\lambda_{max} = 267$ nm, indicative of covalent coupling of the catechol (Fig. 5a and b).[41] Significantly, the aged gels exhibit fundamentally different rheological behavior than the freshly synthesized gels, evident in dynamic oscillatory shear and stress relaxation experiments (Fig. 6 and ESI Fig. S3†). Rather than rapid equilibration to a zero stress state, as seen for the freshly synthesized gel, the aged samples show an extended stress decay profile with ~40% residual stress. The combined mechanical and spectroscopic evidence support the observation that the parent catechol system is prone to oxidation and covalent crosslinking, leading to a shift in properties towards a mixed mode covalent/dynamic gel. This loss of supramolecular character was further corroborated by dissolution studies which clearly show that newly synthesized catechol-based gels quickly dissolve in pH 3 acetic acid buffer (~15 seconds) while aged gels were not dissolved over the course of 4+ months.

To further delineate the relative roles of auto-oxidation and iron-catalyzed oxidation, hydrogels were also synthesized from catechol–Al(III) crosslinks. As Al(III) does not have an available

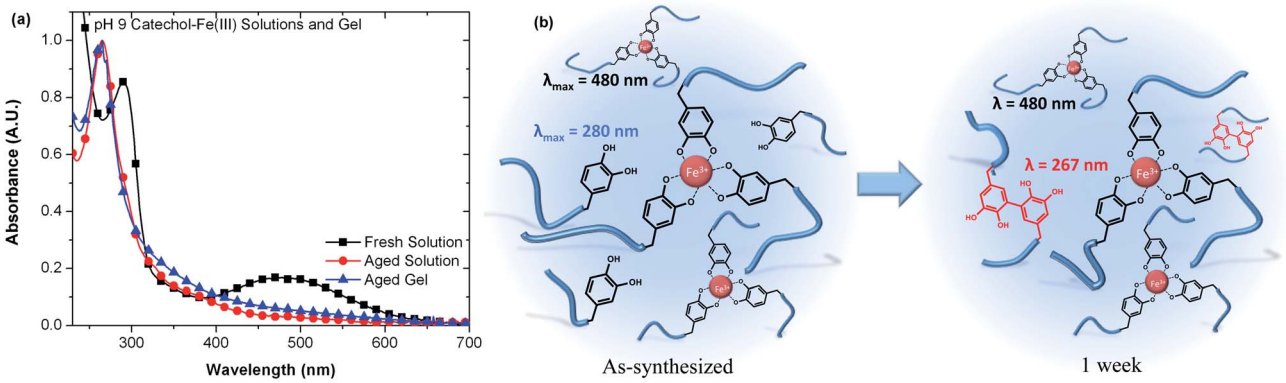

Fig. 5 (a) Absorbance of 1 wt% of catechol–Fe^{3+} crosslinker solutions at pH 9 immediately upon mixing (black squares) and after one week incubation at ambient conditions (red circles), and compared to 10 wt% hydrogel after one week (blue triangles). (b) Schematic depiction of the oxidative crosslinking.

Al(III) state, the one-electron metal-triggered oxidation seen for catechol–Fe(III) cannot occur in this system. In analogy with the catechol–Fe(III) system, the rheological behavior of the catechol–Al(III) gels formed at pH 12 switched from purely dynamic to a mixed mode over the course of a week (ESI Fig. S4†). This variation in rheological properties was accompanied by a change in the color of the gel, from colorless to brown, which was similar to that previously observed for catechol gels crosslinked by chemical oxidation in the absence of Fe(III).[19] From these results it can be concluded that auto-oxidation proceeds even in the presence of strongly tris-chelated catechol species under ambient conditions.

The oxidative instability of the parent catechol systems then prompted an examination of HOPO-based hydrogels with a view to retaining the dynamic, supramolecular properties of these materials. It was therefore pleasing to observe that after 1 month of incubation under ambient conditions, HOPO–Fe(III) gels at pH 9 displayed only minimal change in dynamic oscillatory or stress relaxation behavior (Fig. 6 and ESI Fig. S3†).[42] Further evidence for the lack of covalent crosslinking could be obtained from dissolution studies. Both as-synthesized and aged HOPO gels dissolve in pH 3 buffer (~30 minutes) and almost instantaneously under more acidic conditions, yielding solutions that are spectrophotometrically identical to freshly synthesized solutions at the corresponding pH. Isolation of the 4-arm PEG precursor by Fe/EDTA chelation and centrifuge filtration followed by size exclusion chromatography analysis showed no change in molecular weight or polydispersity.

Influence of different metal ions

Based on the advantages of Fe(III)–HOPO gels described above when compared to traditional catechol systems, the versatility of this design was further explored using additional metal ions which have high affinities for hydroxypyridinone-based ligands.

Al(III) and Ga(III) are trivalent ions with similar atomic radii and tris binding constants to Fe(III). (Fe(III) = 37.2, Al(III) = 32.3, Ga(III) = 38.4)[37] Furthermore, speciation plots for model 3-hydroxy-4-pyridinones predict a similar coordination stoichiometry profile for Fe(III), Al(III) and Ga(III), with predominantly tris complexation at pH 7.4.[43] For comparison, systems based on Cu(II), only capable of mono and bis coordination modes, though with a high binding constant ($\beta_2 = 21.7$)[44] and Gd(III) which has a lower stability constant ($\beta_3 = 17.3$), but is capable of tris chelation, were examined.

HOPO–Al(III) gels were found to form strong hydrogels with slightly shorter bond lifetimes than gels formed with Fe(III), as reflected by step strain (Fig. 7) and dynamic oscillatory experiments (ESI Fig. S4†). In contrast, Ga(III)-based gels showed markedly lower values for plateau moduli and characteristic relaxation time. From a thermodynamics standpoint, Ga(III)-based hydrogels would be expected to exhibit similar characteristics to Fe(III)-based crosslinks, while Al(III) would exhibit less elastic behavior, a result that is contrary to the observed rheology, and suggests that ligand exchange kinetics play a role in the observed mechanical properties. Water exchange rates have generally been used as an approximation of ion lability in ligand exchange reactions in aqueous media. Ga(III) is known to be more labile than Fe(III), which in turn is several orders of magnitude more labile than Al(III).[45] As the observed hydrogel elasticity trends do not correspond to predictions based solely on thermodynamic or kinetic considerations, it appears that the mechanical properties of the hydrogel are determined by a combination of these factors that remain to be explored.

No gelation was seen upon raising the pH of a polymer–Gd(III) bound solution to 7.4, whereas increasing pH beyond this point led to cloudiness in the solution, presumably due to hydrolysis and higher order GdO_x complexes. The fact that this is not observed for higher affinity metal ions, especially Fe(III), which have extremely low solubility at higher pH, highlights the ability of the gels to bind and sequester the metal ions from bulk solution. Finally, gelation with Cu(II) was explored. An initially blue solution turned green upon titration to pH 9, forming a very weak green gel upon pH adjustment to 12. In agreement with this observation, dynamic rheological characterization revealed very short characteristic bond lifetimes with a high plateau modulus at high oscillatory shear frequencies.

Degradation and release properties

These promising properties for HOPO systems then prompted a basic study of the degradation properties of Fe(III)–HOPO gels formed by injection into physiological buffer solution. In assessing potential stability for *in vitro* application, hydrogel samples (150 μL) were incubated in a sealed vial at 37 °C with gentle agitation in the presence of a ten-fold excess of pH 7.4 phosphate buffer solution. The buffer solution was changed regularly, and the characteristic absorbance of the 3 : 1 HOPO–Fe(III) tris-complexes was used to determine polymer concentration in the supernatant. As Fig. 8 shows, gradual polymeric mass loss results in complete dissolution after 4 days. The iron chelation efficacy of the clinically prescribed ligand deferiprone and similar HOPO analogues under biological conditions suggests that the degradation process would not release a substantial amount of Fenton-active Fe(II).[46]

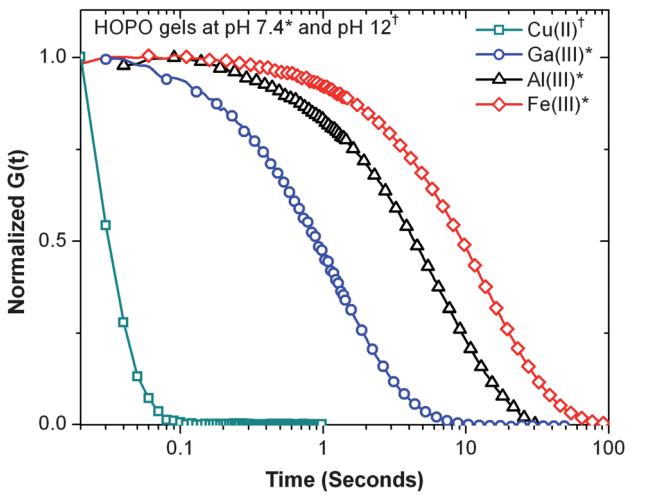

Fig. 7 Effect of metal ion identity on relaxation of HOPO hydrogels sheared by a 20% step strain.

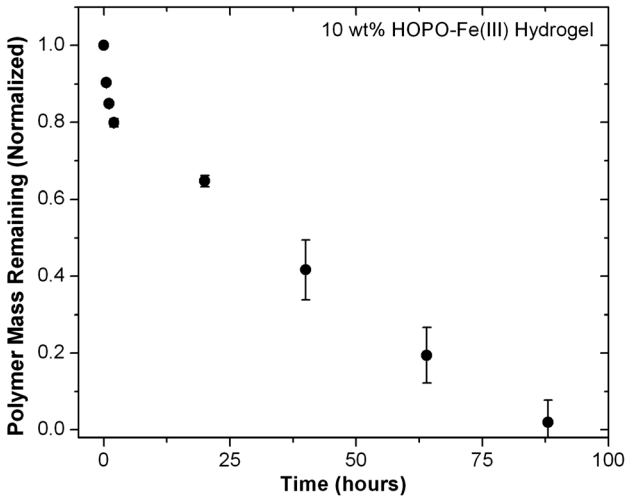

Fig. 8 Degradation of HOPO–Fe(III) hydrogel samples in pH 7.4 buffer at 37 °C ($n = 3$, error bars represent standard deviation).

Finally, the small molecule release profiles were examined for the HOPO-based hydrogels. The water soluble dye Amaranth (Acid Red 27) was selected as a model small molecule drug having no specific interactions with the gel being used, as the tris HOPO crosslinks with trivalent ions carry no charge. The hydrogel was synthesized through the previously described injection strategy, where a 0.4% w/v loading of dye was incorporated into the pre-gel solution. The solution was dropped into pH 7.4 phosphate buffer solution and incubated in a manner consistent with the mass erosion studies, where the buffer solution was changed at the indicated times. The concentration of released dye was determined by measuring the absorbance of the supernatant at 520 nm, and the normalized results are shown in Fig. 9. Hydrogels with HOPO–Al(III) crosslinks were used as these coordination complexes have no absorbance in the analytical range, in comparison to HOPO–Fe(III) complexes, which absorb strongly in this region. Spectroscopic measurements show very high initial incorporation of dye, with just $2.2 \pm 0.5\%$ of the initial dye payload released through the injection and 30 second gelation period. Drug release can be modeled by the Korsmeyer–Peppas equation,

$$\frac{Q_t}{Q} = kt^n$$

where Q_t is the release amount at time t, Q is the total amount released, k is the kinetic constant, and n is the release index. A release index of less than 0.45 indicates a purely Fickian diffusion release mechanism, while a release index between 0.45 and 0.89 indicates a mixed mode release where both diffusion and erosion play a role. A power law fit of the data, shown on Fig. 9 (correlation constant, $R = 0.99$) yields a value for n of 0.49. This implied mixed release mechanism is in agreement with experiment observation, as final dye release occurs concurrently with gel dissolution. As release is controlled in part by hydrogel pore size, release kinetics could conceivably be tuned by changing the distance between crosslinks in gels of this construct.

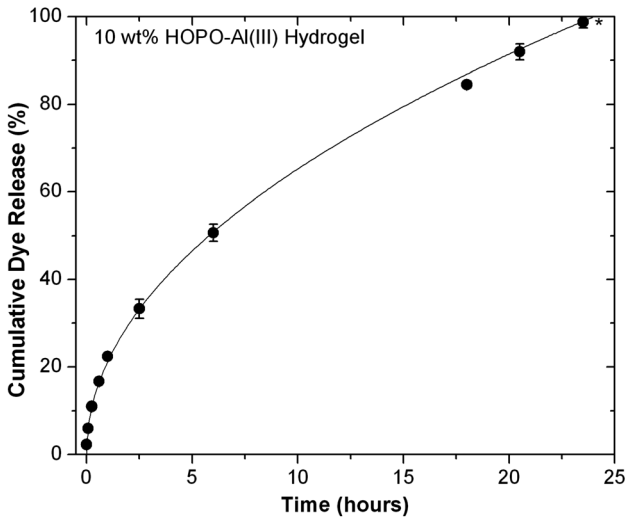

Fig. 9 Dye release profile of Acid Red 27 from HOPO–Al(III) hydrogel into pH 7.4 buffer ($n = 3$, error bars represent standard deviation).

Conclusions

Examination of a number of catechol-based ligands for metal-ion induced hydrogel formation has clearly demonstrated the utility and advantages of HOPO as structural motif and showcases its function in a load-bearing role under biologically mimetic conditions. Hydrogels formed by the chelation of Fe(III) by 4-arm HOPO-terminated polyethylene glycol molecules exhibit several advantages over more traditionally used catechol–Fe(III) chemistry. First, the chelation stoichiometry of HOPO is much better attuned to physiological conditions, allowing almost instantaneous formation of robust gels upon injection into physiological buffer without the need for an external oxidizing agent. Gels encapsulated a model dye compound with high efficiency, and slowly degraded over 4 days in buffer solution, while catechol-based gels could not be formed in this manner. Second, whereas the catechol–Fe(III) complex is shown to be vulnerable to oxidative covalent crosslinking under a wide variety of conditions, HOPO–Fe(III) hydrogels were found to maintain robust, dynamic crosslinking and subsequently stable rheological properties over the course of months. Finally, HOPO is a versatile metal binding species, capable of gelation at physiological pH with Al(III) and Ga(III), and at higher pH with Cu(II) metal ions.

Experimental

Materials

Chemicals were purchased from Sigma Aldrich and used as received. 6-Nitrodopamine was synthesized following a previously published method.[33] 1-(2′-Aminoethyl)-2-methyl-3-hydroxy-4-pyridinone dihydrochloride (HOPO) was synthesized following the procedure of Dobbin *et al.*[31] 4-arm PEG–OH (MW: 10 000 Da) was purchased from Nanocs, Inc. *N*,*N*-Dimethylformamide (DMF) and dichloromethane (DCM) were collected directly from a solvent purification system (PureSolv,

Innovative Technology). Deuterated solvents were obtained from Cambridge Isotope Laboratories, Inc.

Instrumentation

^{1}H and ^{13}C NMR spectra were recorded using a Varian 600 MHz spectrometer with the solvent signal as internal reference. Gel permeation chromatography (GPC) was performed on a Waters 2690 separation module equipped with Waters 2414 refractive index and 2996 photodiode array detectors using $CHCl_3$ containing 0.25% triethylamine as eluent at a flow rate of 1 mL min^{-1}. Molecular weight distributions (PDIs) were calculated relative to linear poly(ethylene oxide) standards. ESI mass spectrometry was performed on a Micromass QTOF2 quadrupole/time-of-flight tandem mass spectrometer. UV-Vis spectra were recorded on an Agilent 8453 spectrophotometer using quartz cuvettes with 1 cm path length and blanked against the relevant buffer solution.

Methods

Synthesis of 4-arm PEG–COOH. A solution of 10 kDa 4-arm PEG–OH (2.14 g, 0.856 mmol –OH) in toluene (50 mL) was azeotropically dried by removal of 10 mL of solvent. A mixture of *tert*-butanol (2 mL) and potassium *tert*-butoxide (0.192 g, 1.712 mmol, 2 EQ/OH) was added to the solution and stirred for 3 hours at 50 °C. Ethyl bromoacetate (380.7 mL, 3.424 mmol, 4 EQ/–OH) was added, and the mixture was stirred overnight at 50 °C under an inert atmosphere. The solvent was removed *in vacuo* and the residue was redissolved in 1 M NaOH (10 mL) and stirred for 4 hours to hydrolyze the ethyl ester. The pH was then adjusted to 1.5 with 1 M HCl, and the product extracted with dichloromethane, dried with anhydrous sodium sulfate, concentrated and precipitated in cold ether. The precipitated product was filtered and dried under reduced pressure, to yield 2.01 g of white powder. NMR ($CDCl_3$): 3.41 ppm (s, C–*CH_2*–O, 8H), 4.16 ppm (s, *CH_2*–COOH, 8H), 98% functionalization.

Synthesis of 4-arm PEG–chelators. PEG–$(COOH)_4$ (500 mg, 0.2 mmol –COOH) was dissolved in 4 mL of a degassed 50/50 mixture of DCM and DMF with the desired chelator amine (0.4 mmol), HOBt (1-hydroxybenzotriazole) (108 mg, 0.8 mmol), and triethylamine (139.5 μL, 1 mmol) to form a cloudy solution. [2-(1*H*-Benzotriazol-1-yl)-1,1,3,3-tetramethyluronium hexafluorophosphate] (HBTU) (151.8 mg, 0.4 mmol) in 2 mL of dry dichloromethane was added, and the coupling reaction was carried out under argon at room temperature for 1 hour. The solution was concentrated, redissolved in 0.5 M HCl (10 mL), and then purified *via* centrifuge dialysis (2 × 15 mL pH 3 HCl, 2 × 15 mL MilliQ water, 5000*g*, 20 min, MWCO: 3 kDa). Freeze drying gave the desired PEG–$(chelator)_4$ as a fluffy white powder.

PEG–$(catechol)_4$ NMR ($CDCl_3$): 2.70 (t, *CH_2*–CH_2–NH–C═O, 8H), 3.41 ppm (s, C–*CH_2*–O, 8H), 3.93 (s, *–CH_2*–CO–NH–CH_2–, 8H), 6.57–6.82 (m, Ar–H, 12H), 90% functionalization, 90% yield.

PEG–$(nitrocatechol)_4$ NMR ($CDCl_3$): 3.01 (t, *CH_2*–CH_2–NH–C═O, 8H), 3.41 ppm (s, C–*CH_2*–O, 8H), 3.95 ppm (s, *–CH_2*–CO–NH–CH_2–, 8H), 6.96 (s, Ar–H, 4H), 7.88 (s, Ar–H, 4H), 95% functionalization, 87% yield.

PEG–$(HOPO)_4$ NMR ($CDCl_3$): 2.68 (s, *CH_3*–Ar, 12H), 3.41 ppm (s, C–*CH_2*–O, 8H), 3.95 ppm (s, *–CH_2*–CO–NH–CH_2–, 8H), 4.42 (t, CH_2–*CH_2*–NH–C═O, 8H), 7.07 (s, Ar–*H*, 4H), 7.96 (s, Ar–H, 4H), 96% functionalization, 92% yield.

Formation of hydrogels

"Dilution" gelation followed a slightly modified version of the procedure established by Holten-Andersen *et al.*[19] Briefly, a 200 μL 10% w/v hydrogel was made by dissolving 20 mg of the relevant 4-arm crosslinker in a minimum amount (25 μL) of unbuffered Milli-Q water. To this solution was added 10 μL of a 0.19 mM $FeCl_3 \cdot 6H_2O$ solution to achieve a chelator : Fe(III) ratio of 3 : 1. Finally, the hydrogel was formed by addition of 120 mM buffer solution (165 μL). This buffer addition was verified to yield the desired hydrogel pH by determination with a pH probe electrode.

"Injection" gelation followed the same initial dissolution and $FeCl_3$ binding steps. This iron-bound polymer solution was diluted with unbuffered Milli-Q water to achieve 200 μL of solution which remained below the gel point for all chelators (pH $\sim$ 3). This solution was dropped or injected into a 3 mL reservoir of the desired 120 mM buffer solution. In the case of Fe(III)–HOPO solutions into pH 7.4 phosphate buffer or pH 9 bicarbonate buffer, distinct gelation was immediately apparent.

Dynamic rheology

Rheological experiments were performed on a Rheometrics Scientific ARES II rheometer with parallel plate geometry (25 mm or 8 mm diameter rotating top plate) at 23 °C. Initial time sweeps were carried out (1% strain, 1 Hz) to ensure gel equilibration, and further rheological testing proceeded only after a stable G' value had been achieved (up to 10 minutes for highly elastic hydrogels). Strain sweep experiments (1 Hz) determined the linear viscoelastic region to extend to 30–50% strain for all hydrogels tested. Oscillatory shear testing of gels as a function of frequency was performed using 5% strain. Characteristic relaxation time, τ, was determined as the inverse of the crossover frequency of the storage (G') and loss (G'') moduli. Step strain testing was performed by applying a 20% strain and monitoring the relaxation modulus $G(t)$. Initial relaxation modulus values were normalized to allow comparison between hydrogels of different pH, chelator and metal ion identity. Sample dehydration was minimized through the use of an enclosed, humidified chamber during testing. Data points represent the average of testing on two separate gels each measured in duplicate.

Hydrogel dissolution studies

150 μL HOPO–Fe(III) hydrogel samples ($n = 3$) were placed in a 2 mL vial on a shaker in a 37 °C incubator. The gels were covered with 1.5 mL of 0.12 M phosphate buffer solution (pH 7.4) and gently shaken. The supernatant was collected every 30 minutes for the first 2 hours, and once a day thereafter. The gels were patted dry and weighed, and the supernatant was subjected to

UV-Vis. Reference 4-arm HOPO–Fe(III) solutions allowed the determination of molar absorptivities for the HOPO ligand (272 nm, $\varepsilon = 8010\ M^{-1}\ cm^{-1}$) and the charge transfer absorbance (460 nm, $\varepsilon = 653\ M^{-1}\ cm^{-1}$). The concentration of the 4-arm chelator complex in the supernatant was determined by measurement of these absorbances, and used to calculate the mass of hydrogel remaining.

Small molecule release studies

Samples for small molecule release studies were synthesized in a manner analogous to the "injection" gelation strategy outlined above. 150 μL of a 10% w/v "pre-gel" solution was prepared by dissolving 15 mg of 4-arm PEG–HOPO in 102 μL of Acid Red 27 dye solution (0.66 mg, 0.4 μmol) in deionized water and 48 μL of $AlCl_3$ solution to achieve a 3 : 1 chelator : Al^{3+} stoichiometry. This dark red solution was injected in 50 μL aliquots into 1 mL reservoirs of 120 mM PBS buffer (pH 7.4), leading to immediate gelation. The supernatant was removed after 30 seconds of setting and the gels were centrifuged to collect at the bottom of 1.5 mL Eppendorf tubes. The samples were then covered with 0.5 mL of fresh pH 7.4 buffer solution. Samples were incubated with gentle shaking. At the times indicated, the supernatant was removed and replenished. The concentration of eluted dye was determined by measuring the absorbance at 520 nm.

Acknowledgements

This work was supported by the Materials Research Science and Engineering Centers Program of the National Science Foundation under Award no. DMR 1121053 and the National Institutes of Health under Grant R01-DE018468.

Notes and references

1 H. Li, W. A. Linke, A. F. Oberhauser, M. Carrion-Vazquez, J. G. Kerkvliet, H. Lu, P. E. Marszalek and J. M. Fernandez, *Nature*, 2002, **418**, 998–1002.
2 N. Becker, E. Oroudjev, S. Mutz, J. P. Cleveland, P. K. Hansma, C. Y. Hayashi, D. E. Makarov and H. G. Hansma, *Nat. Mater.*, 2003, **2**, 278–283.
3 E. A. Appel, J. del Barrio, X. J. Loh and O. A. Scherman, *Chem. Soc. Rev.*, 2012, **41**, 6195–6214.
4 P. Lundberg, N. A. Lynd, Y. Zhang, X. Zeng, D. V. Krogstad, T. Paffen, M. Malkoch, A. M. Nyström and C. J. Hawker, *Soft Matter*, 2013, **9**, 82–89.
5 M. Krogsgaard, M. A. Behrens, J. S. Pedersen and H. Birkedal, *Biomacromolecules*, 2013, **14**, 297–301.
6 B. Jeong, Y. H. Bae, D. S. Lee and S. W. Kim, *Nature*, 1997, **388**, 860–862.
7 R. Zhang, M. Tang, A. Bowyer, R. Eisenthal and J. Hubble, *Biomaterials*, 2005, **26**, 4677–4683.
8 L. A. Haines, K. Rajagopal, B. Ozbas, D. A. Salick, D. J. Pochan and J. P. Schneider, *J. Am. Chem. Soc.*, 2005, **127**, 17025–17029.
9 Z. Shafiq, J. Cui, L. Pastor-Pérez, V. San Miguel, R. A. Gropeanu, C. Serrano and A. del Campo, *Angew. Chem., Int. Ed.*, 2012, **51**, 4332–4335.
10 (*a*) M. Burnworth, L. Tang, J. R. Kumpfer, A. J. Duncan, F. L. Beyer, G. L. Fiore, S. J. Rowan and C. Weder, *Nature*, 2011, **472**, 334–337; (*b*) J. Kumpfer and S. Rowan, *J. Am. Chem. Soc.*, 2011, **133**, 12866–12874.
11 S. Matsumoto, S. Yamaguchi, S. Ueno, H. Komatsu, M. Ikeda, K. Ishizuka, Y. Iko, K. V. Tabata, H. Aoki, S. Ito, H. Noji and I. Hamachi, *Chem.–Eur. J.*, 2008, **14**, 3977–3986.
12 H. Komatsu, S. Matsumoto, S. Tamaru, K. Kaneko, M. Ikeda and I. Hamachi, *J. Am. Chem. Soc.*, 2009, **131**, 5580–5885.
13 J. Cui and A. del Campo, *Chem. Commun.*, 2012, **48**, 9302–9304.
14 R. P. Sijbesma, F. H. Beijer, L. Brunsveld, B. J. B. Folmer, J. H. K. K. Hirschberg, R. F. M. Lange, J. K. L. Lowe and E. W. Meijer, *Science*, 1997, **278**, 1601–1604.
15 D. C. Tuncaboylu, M. Sari, W. Oppermann and O. Okay, *Macromolecules*, 2011, **44**, 4997–5005.
16 S. Burattini, B. W. Greenland, D. H. Merino, W. Weng, J. Seppala, H. M. Colquhoun, W. Hayes, M. E. Mackay, I. W. Hamley and S. J. Rowan, *J. Am. Chem. Soc.*, 2010, **132**, 12051–12058.
17 Q. Wang, J. L. Mynar, M. Yoshida, E. Lee, M. Lee, K. Okuro, K. Kinbara and T. Aida, *Nature*, 2010, **463**, 339–343.
18 J. N. Hunt, K. E. Feldman, N. A. Lynd, J. Deek, L. M. Campos, J. M. Spruell, B. M. Hernandez, E. J. Kramer and C. J. Hawker, *Adv. Mater.*, 2011, **23**, 2327–2331.
19 N. Holten-Andersen, M. J. Harrington, H. Birkedal, B. P. Lee, P. B. Messersmith, K. Y. C. Lee and J. H. Waite, *Proc. Natl. Acad. Sci. U. S. A.*, 2011, **108**, 2651–2655.
20 (*a*) D. E. Fullenkamp, L. He, D. G. Barrett, W. R. Burghardt and P. B. Messersmith, *Macromolecules*, 2013, **46**, 1167–1174; (*b*) Z. Li, L. E. Buerkle, M. R. Orseno, K. A. Streletzky, S. Seifert, A. M. Jamieson and S. J. Rowan, *Langmuir*, 2010, **26**, 10093–10101.
21 P. J. Knerr, M. C. Branco, R. Nagarkar, D. J. Pochan and J. P. Schneider, *J. Mater. Chem.*, 2012, **22**, 1352–1357.
22 W. C. Yount, D. M. Loveless and S. L. Craig, *J. Am. Chem. Soc.*, 2005, **127**, 14488–14496.
23 K. N. Raymond, E. A. Dertz and S. S. Kim, *Proc. Natl. Acad. Sci. U. S. A.*, 2003, **100**, 3584–3588.
24 M. J. Harrington, A. Masic, N. Holten-Andersen, J. H. Waite and P. Fratzl, *Science*, 2010, **328**, 216–220.
25 E. Herlinger, R. F. Jamesonb and W. Linerta, *J. Chem. Soc., Perkin Trans. 2*, 1995, **2**, 259–263.
26 B. P. Lee, J. L. Dalsin and P. B. Messersmith, *Biomacromolecules*, 2002, **3**, 1038–1047.
27 H. G. Jang, D. D. Cox and L. Que, *J. Am. Chem. Soc.*, 1991, **113**, 9200–9204.
28 T. Kawabata, V. Schepkin, N. Haramaki, R. S. Phadke and L. Packer, *Biochem. Pharmacol.*, 1996, **51**, 1569–1577.
29 D. G. Barrett, D. E. Fullenkamp, L. He, N. Holten-Andersen, K. Y. C. Lee and P. B. Messersmith, *Adv. Funct. Mater.*, 2012, **23**, 1111–1119.
30 V. M. Nurchi, T. Pivetta, J. I. Lachowicz and G. Crisponi, *J. Inorg. Biochem.*, 2009, **103**, 227–236.

31 P. S. Dobbin, R. C. Hider, A. D. Hall, P. D. Taylor, P. Sarpong, J. B. Porter, G. Xiao and D. van der Helm, *J. Med. Chem.*, 1993, **36**, 2448–2458.
32 M. P. Lutolf, J. L. Lauer-Fields, H. G. Schmoekel, A. T. Metters, F. E. Weber, G. B. Fields and J. A. Hubbell, *Proc. Natl. Acad. Sci. U. S. A.*, 2003, **100**, 5413–5418.
33 A. Napolitano, A. Palumbo and M. d'Ischia, *Tetrahedron*, 2000, **56**, 5941–5945.
34 B. Mizrahi, S. A. Shankarappa, J. M. Hickey, J. C. Dohlman, B. P. Timko, K. A. Whitehead, J. J. Lee, R. Langer, D. G. Anderson and D. S. Kohane, *Adv. Funct. Mater.*, 2012, **23**, 1527–1533.
35 J. N. Israelachvili, in *Intermolecular and Surface Forces*, Elsevier, Burlington, MA, 3rd edn, 2011, Part 1, ch. 9, pp. 169–188.
36 B. Monzyk and A. L. Crumbliss, *J. Am. Chem. Soc.*, 1982, **104**, 4921–4929.
37 J. Burgess and M. Rangel, *Adv. Inorg. Chem.*, 2008, **60**, 167–243.
38 T. Zhou, Y. Ma, X. Kong and R. C. Hider, *Dalton Trans.*, 2012, **41**, 6371–6389.
39 V. M. Nurchi, G. Crisponi, T. Pivetta, M. Donatoni and M. Remelli, *J. Inorg. Biochem.*, 2008, **102**, 684–692.
40 K. T. Finley, in *Chemistry of the Quinonoid Compounds*, ed. S. Patai, Wiley, London, 1974, vol. 2, ch. 17, p. 878.
41 S. Olav, J. P. Jacobsen, G. Bojesen and P. Roepstorff, *Biochim. Biophys. Acta*, 1992, **1118**, 134–138.
42 H. Yadegari, A. Jabbari, H. Heli, A. Moosavimovahedi, K. Karimian and A. Khodadadi, *Electrochim. Acta*, 2008, **53**, 2907–2916.
43 M. A. Santos, M. Gil, L. Gano and S. Chaves, *JBIC, J. Biol. Inorg. Chem.*, 2005, **10**, 564–580.
44 A. El-Jammal, P. L. Howell, M. A. Turner, N. Li and D. M. Templeton, *J. Med. Chem.*, 1994, **37**, 461–466.
45 L. Helm and A. E. Merbach, *Coord. Chem. Rev.*, 1999, **187**, 151–181.
46 M. Merkofer, R. Kissner, R. C. Hider, U. T. Brunk and W. H. Koppenol, *Chem. Res. Toxicol.*, 2006, **19**, 1263–1269.